Does Chiral Sensitivity of a Structure Depend on the Metal Core? Alkali Ion Complexes of Cyclo(Tyr-Tyr)

Koki Yoshizawa, Keisuke Hirata, Shun-ichi Ishiuchi, Masaaki Fujii, Anne Zehnacker

Does Chiral Sensitivity of a Structure Depend on the Metal Core? Alkali Ion Complexes of Cyclo(Tyr-Tyr)

Koki Yoshizawa,[1,2] Keisuke Hirata,[1,3] Shun-ichi Ishiuchi,[1,3*] Masaaki Fujii,[1,2,4*] Anne Zehnacker,[4,5*] [i]

[1]*Laboratory for Chemistry and Life Science, Institute of Innovative Research, Tokyo Institute of Technology, 4259, Nagatsuta-cho, Midori-ku, Yokohama, 226-8503, Japan*

[2]*School of Life Science and Technology, Tokyo Institute of Technology. 4259 Nagatsuta-cho, Midori-ku, Yokohama, Kanagawa, 226-8503, Japan.*

[3]*Department of Chemistry, School of Science, Tokyo Institute of Technology, 2-12-1 Ookayama, Meguro-ku, Tokyo 152-8550, Japan.*

[4]*International Research Frontiers Initiative (IRFI), Institute of Innovative Research, Tokyo Institute of Technology, 4259, Nagatsuta-cho, Midori-ku, Yokohama, Japan*

[5]*Institut des Sciences Moléculaires d'Orsay (ISMO), CNRS, Université Paris-Saclay, F-91405 Orsay, France*

* Corresponding authors: anne.zehnacker-rentien@universite-paris-saclay.fr, ishiuchi.s.aa@m.titech.ac.jp, mfujii@res.titech.ac.jp

Abstract

Alkali metal complexes of the cyclic dipeptide cyclo Tyr-Tyr have been studied under cryogenic ion trap conditions. Their structure was obtained by combining Infra-Red Photo-Dissociation (IRPD) and quantum chemical calculations. The structural motif strongly depends on the relative chirality of the tyrosine residues. For residues of identical chirality, the cation interacts with one amide oxygen and one of the aromatic rings only; the distance between the aromatic rings does not change with the nature of the metal. In contrast, for residues of opposite chirality, the metal cation is located in-between the two aromatic rings and interacts with both of them. The distance between the two aromatic rings strongly depends on the metal. Electronic spectra obtained by Ultra Violet Photodissociation (UVPD) spectroscopy and analysis of the UV photo-fragments shed light on the excited state deactivation processes, which depend on both the chirality of the residue and the metal ion core. Na^+ stands out by the presence of low-lying charge transfer states resulting in the broadening of the electronic spectrum.

[i] Mr. Koki Yoshizawa, Dr. Keisuke Hirata, Pr. Shun-ichi Ishiuchi, Pr. Masaaki Fujii, Dr. Anne Zehnacker

Introduction

The excited electronic states of systems containing two or more aromatic chromophores often display a complex structure due to the coupling between them. Exciton splitting is dominant in symmetrical bi-chromophore systems such as the 2-pyridine dimer, where the $S_1 \leftarrow S_0$ transition is forbidden by symmetry and the $S_2 \leftarrow S_0$ transition allowed, and involves important vibronic effects.[1, 2] In complex systems, analysis of the splitting gives information on the distance between the chromophores and their relative orientation.[3] However, dissymmetry brought by substitution or complexation results in a site splitting that often dominates the electronic spectrum.[1, 4] Dissymmetric structures are in particular observed for bi-chromophoric cyclic di-peptides of the diketopiperazine family containing two aromatic amino acids residues of identical or opposite chirality. Diketopiperazine (DKP) peptides are cyclic di-peptides produced by intramolecular amide bond formation in a linear peptide. Their cyclic nature endows them with high stability due to the absence of C or N terminus group and with limited conformational flexibility. Therefore, their rigidity and stability make them interesting scaffold for the synthesis of innovative drugs.[5, 6] From the fundamental point of view, they provide model systems for studying the influence of the chirality of the residues on the structure of sterically constrained systems. We have undertaken a study of DKP dipeptides containing at least one aromatic amino acid under jet-cooled or ion trap conditions.[7-16] Among the studied systems, those containing two aromatic amino-acids are of special interest as they raise the question of the localisation of the electronic transition and the coupling between the two aromatic chromophores (see Figure 1). The most stable structures of neutral bi-chromophore DKP dipeptides, like cyclo(phenylalanyl-phenylalanyl) (c-Phe-Phe) or cyclo(phenylalanyl-tyrosyl) (c-Phe-Tyr),[10, 14, 15] are very similar, although spectroscopically discernible, whether the two residues have identical or opposite absolute configurations. Double resonance IR-UV experiments under jet-cooled conditions points towards a dissymmetric structure.[10, 14, 15, 17] In the most stable form, one of the aromatic rings is folded over the DKP ring while the other one is extended outwards (Figures 1c and 1d). This results in the localisation of the electronic transitions. The lower-energy transition $S_1 \leftarrow S_0$ is localised on the extended aromatic ring while $S_2 \leftarrow S_0$ is localised on the folded ring. Cyclo(tyrosyl-tyrosyl) stands out in that an additional structure is observed for residues of identical absolute configuration, with the two phenol rings in a stacked geometry, resulting in a broad electronic absorption.[17] This structure is stabilised by an intramolecular hydrogen bond between the two phenolic OH groups, which overcomes the repulsion between the aromatic rings (Figure 1c'). Still, the first two electronic transitions are localised on each aromatic ring. Protonation of the molecule happens on the amide CO and destabilises the stacked geometry to the benefit of a folded-extended structure stabilised by the interaction between the OH^+ group and the extended ring, shown in Figures 1e and 1f. Despite the perturbation brought by the point charge and the dominant $OH^+ \ldots \pi$ interaction, the two diastereomers are still clearly distinguishable by their spectroscopic signature in the 3 μm region.[7] The study of ion-core complexes of DKP peptides with alkali metals is still scarce.[18] Due to the cyclic nature of the DKP dipeptides, no charge-solvated structure can be formed, in contrast to linear peptides.[19] Steric constraints also prevent formation of NH…O hydrogen bonds that could compete with the M^+...O interaction. Therefore, only the amide CO and the

aromatic rings are expected to compete for binding the metal, which makes the system simpler than linear peptides. The competition between the aromatic rings and the amide CO depends on both the peptide sequence[20] and the ionic radius of the ion.[21] For the protected Ac-Tyr-NHMe peptide for example, built on the glycine-tyrosine-glycine sequence, the tridentate conformation where the metal interacts with two amide oxygen atoms and the aromatic ring (OOπ) is preferred for all the alkali metal ions complexes at 0K. At room temperature, however, while OOπ is still the most stable for Li^+ or Na^+, larger alkali cations prefer the bidentate conformation in which the cation only interacts with the two amide oxygen atoms (OO).[21] This points towards important entropic effects in this kind of systems. Open structures are favoured for the alkali ions complexes of bi-chromophore phenylalanyl-phenylalanyl dipeptides with alkali ions, with the two aromatic rings in a fully extended conformation to minimise repulsion between them.[22] In these structures, the alkali metal ion interacts with two amide oxygen atoms and one aromatic ring only (OOπ). Only divalent ions like Ca^{2+} form very compact complexes where the ion is sandwiched between the two aromatic rings in a tetravalent fashion (OO$\pi\pi$).[22] Stereochemical factors also are important to define the interaction mode and shape the molecular structure.[15, 23] The Li^+ or Na^+ core diphenylalanine complexes have an OOπ structural pattern when the two residues are of opposite absolute configuration. When they have identical absolute configuration, interaction with one the N terminal nitrogen atom (OON) is energetically competitive with the OOπ geometry. Also the structure of the tetra phenylalanine Na^+ complex depends on chirality; the all L peptide showing an OO$\pi\pi$ interaction pattern and the LDLD peptide an OOOOπ scheme.[24]

In this work, we extend our study on the cyclo-(tyrosyl-tyrosyl) dipeptide to its ion-core complexes, for a series of alkali metal ions ranging from Li^+ to Cs^+. We aim to understand whether the relative chirality of the residues influences the binding pattern of the metal ion, the nature of the excited state and the photophysical processes resulting from UV excitation. In addition, we study whether the structure of the ground and first electronic excited states as well as the nature of the photofragments depend on the size of the metal ion. To this end, we use action spectroscopy under cryogenic ion trap conditions, both in the IR and UV range, together with quantum chemical calculations. The studied molecule is shown in Figure 1. In what follows, the ion-core complexes will be denoted c-LL-M^+ and c-LD-M^+, with M standing for Li, Na, K, Rb, Cs, respectively.

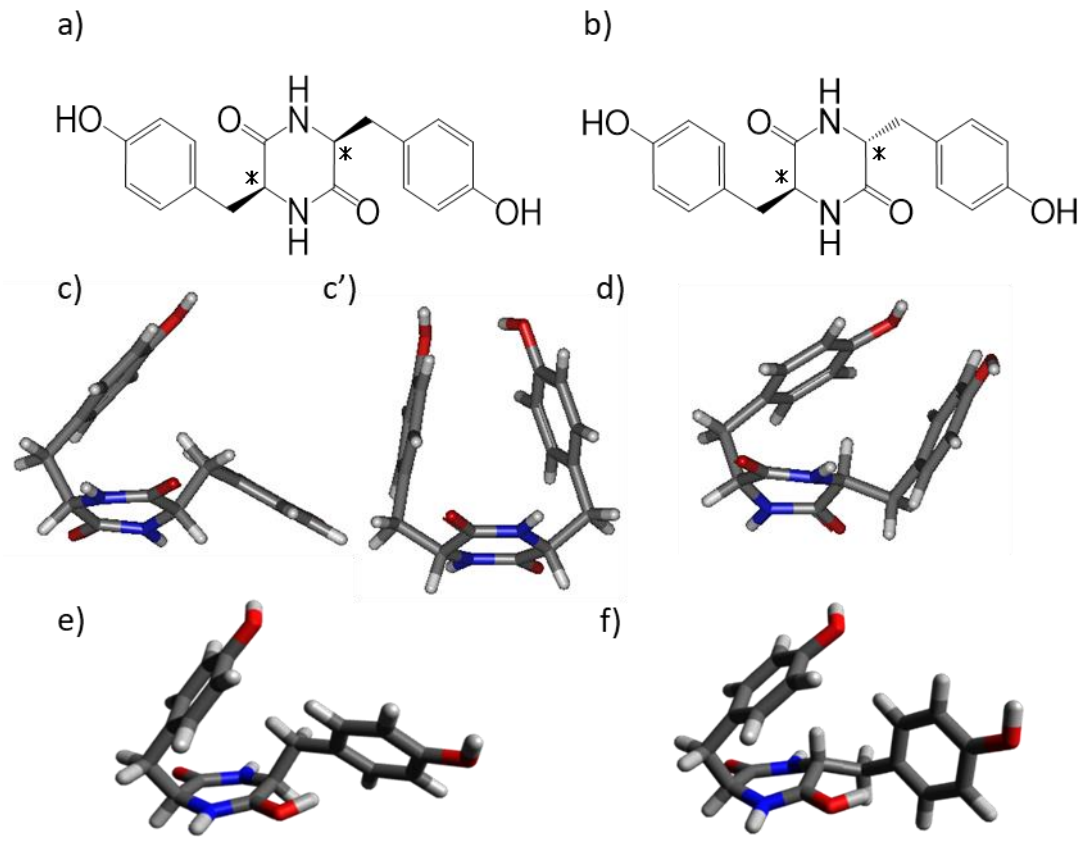

Figure 1: Scheme of the studied molecule. a) cyclo (tyrosyl-tyrosyl) (c-LL) b) cyclo (tyrosyl-D-tyrosyl) (c-LD). The stereogenic centres are shown with *. c) and c') most stable forms of neutral c-LL d) most stable form of neutral c-LD. e) and f) most stable structures of c-LLH$^+$ and c-LDH$^+$, respectively.

Experimental Section

Experimental Methods

Cyclo Tyr-Tyr (>99%) was purchased from Genecust (Luxembourg), and used without further purification. The experimental set-up has been described in detail already.[25] Briefly, the methanol solutions containing cyclo(Tyr-Tyr) at a concentration of 1.2×10^{-5} ML^{-1} and the cation at a concentration of 1×10^{-4} ML^{-1} were electro-sprayed from a nebulizer. The droplets were evaporated by travelling through a glass capillary heated up to 80^{o}C. The ions efficiently collected by an ion funnel were injected into a quadrupole mass spectrometer (Q-MS: Extrel) via a hexapole ion guide. The target complex was mass selected by the Q-MS and then introduced to a cryogenic quadrupole ion trap (QIT) via a quadrupole ion bender and octupole ion guides. The QIT was kept at 4K by a closed-cycle two-stage He cryostat (Sumitomo: RDK-408D2) during the whole experiment. A mixed buffer gas of H_2 (20%) and helium was introduced to the QIT using a pulsed valve (Parker Hannifin: General Valve Series 9). The mass-selected ions were allowed to collide with the cold buffer gas so that they were trapped in the QIT and cooled down to ~10K. Hydrogen molecules weakly attached to the ions under such cryogenic conditions. The H_2-tagged ions were irradiated in the cold trap with a tuneable IR

laser (LaserVision: OPO/OPA). Hydrogen molecules were detached from the cluster ions when the wavenumber of the IR laser was resonant to a vibrational transition of the cluster ions.[26] The photofragments were extracted linearly and detected by a linear time-of-flight mass spectrometer (TOFMS). The photofragment ion signals from a dynode converter detector of TOFMS were amplified 10 times by a preamplifier and recorded on a fast digitizer. IR photodissociation (IRPD) spectra were measured by monitoring the intensity of the photofragments resulting from H_2 loss, *i.e.* the ion core complex, as a function of the wavenumber of the IR laser. The UV photodissociation spectra (UVPD) of the trapped ions was measured by monitoring the fragment intensity (*vide infra)* as a function of the wavenumber of the UV laser. The UV light source was the frequency-doubled output of a dye laser (Sirah, Cobra Stretch) pumped by the third harmonic of a Nd:YAG laser (Spectra Physics).

Theoretical Methods

The geometry of the Li^+, Na^+ and K^+ ion core complexes were optimised at the B3LYP/6-311++G(d,p) level, including the D3 dispersion corrections,[27-29] as done previously for the neutral and protonated molecules.[7, 17] The LANL2DZ pseudo potential was used for Rb^+ and Cs^+, keeping the 6-311++g(d,p) basis set for the C, N, O and H atoms. The harmonic frequencies were calculated at the same level of theory. The frequencies were scaled by 0.952 in the 3 μm region and 0.978 in the fingerprint region. All calculations were performed with the Gaussian Package (Version 16 Rev. B.01).[30] The starting structures were those used for the protonated system, replacing the proton by the metal ion.[7] Only one of the phenolic OH orientations was kept, due to the very small difference in energy and vibrational spectrum between the two orientations.
The electronic excited states of the metal core complexes were calculated at the ri-cc2 level of theory, using the resolution-of-the-identity (ri) approximation.[31] To this end, the ground-state structures obtained at the DFT level were re-calculated at the ri-cc2 level using the TZVP basis set for the Li^+, Na^+, K^+ complexes and the def2-SVP basis set together with the def2-ecp pseudo potential for the Rb^+ and Cs^+ complexes. The vertical excitation energies were calculated at the ri-cc2 level, with six excited states. The changes in electronic densities between the ground state and the electronic excited states were calculated at the same level of theory and plotted using the VMD software, with an isodensity value of 0.001.[32]

Results and Discussion

Vibrational Spectroscopy In the 3 μm Region and Structural Assignments

The experimental vibrational spectra in the region of 3 μm are shown in Figure 2, as well as the most stable calculated structures and the corresponding simulated spectra. For each complex, the three lower-energy structures as well as their simulated spectra are shown in Figures S1 to S5 of the electronic supplementary information (ESI). Four bands are expected in this region, namely, two ν(OH) and two ν(NH) stretches. As seen in Figure 2, the position of these bands depends on both the metal cation and the relative chirality of the residues.

While the two ν(OH) frequencies are identical for all c-LD-M^+ complexes, a splitting is observed in the c-LL-M^+ complexes, which depends on the cation. The splitting is maximal for Li^+, then decreases to zero for K^+, and remains small for larger metal cations. The variations are more

pronounced for the ν(NH) frequencies. For the c-LL-M^+ ion core complexes, the splitting is maximum for Li^+ and then decreases monotonously to zero, reflecting the increasing distance between the metal ion and the amide (see Figure 3). For the c-LD-M^+ metal complexes, the splitting is small for Li^+, zero for Na^+ and then increases.

An excellent agreement is obtained between the experimental spectra and those simulated for the most stable calculated structures shown in Figure 2. Both evolution of the splitting with the ionic radius and difference between c-LL-M^+ and c-LD-M^+ are well accounted for by the calculations. Based on their relative energy and/or on their simulated spectra, we can discard the higher-energy structures. The most important geometrical parameters of the most stable complexes are summarised in Figure 3. In all these structures, the metal cation is interacting with one of the amide CO, with an M^+…OC distance increasing monotonously with the ionic radius or the polarizability of the metal cation (see Figure 3). This distance does not depend on chirality and is very similar for c-LL-M^+ and c-LD-M^+ for a given ion.

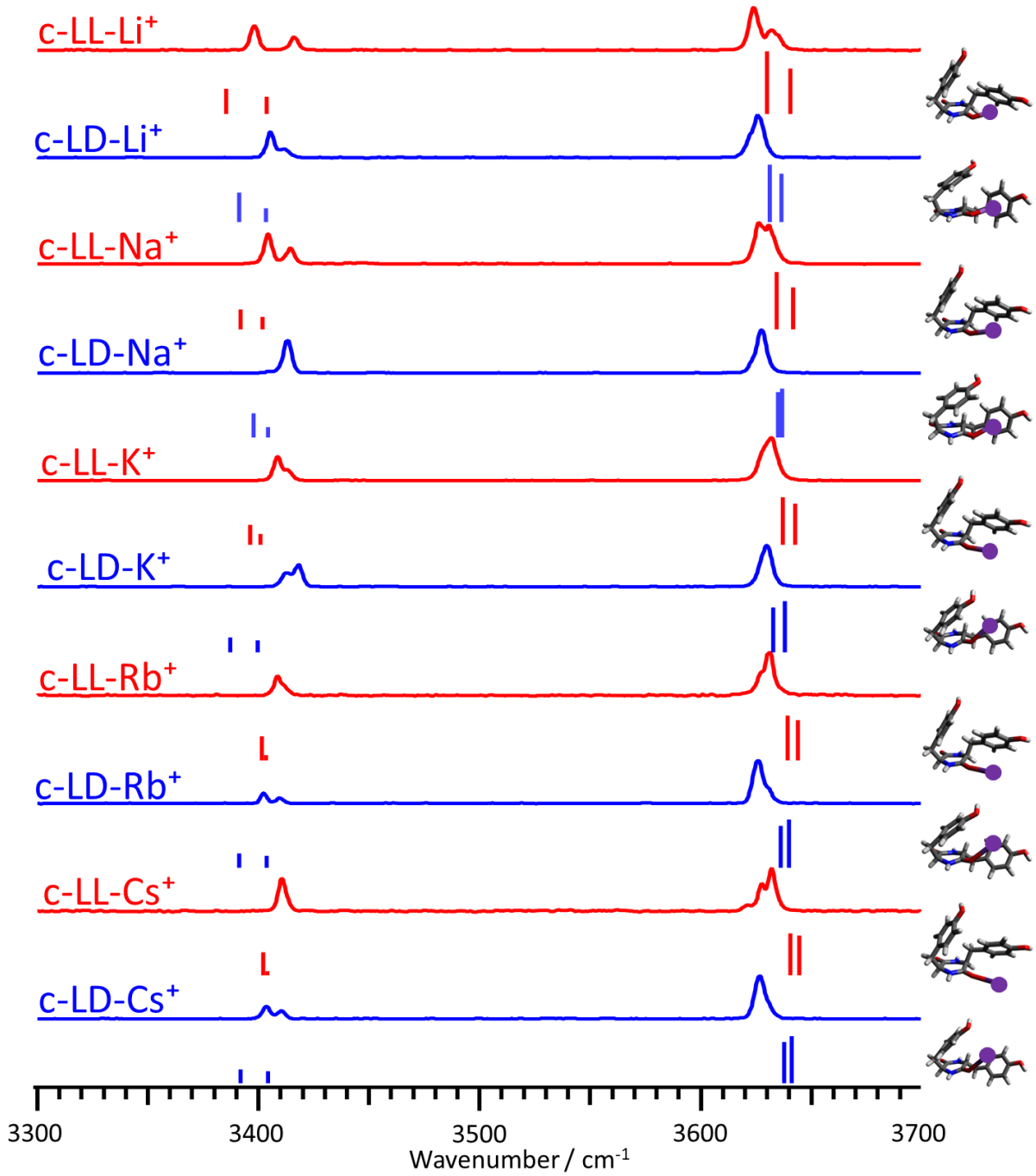

Figure 2: IRPD spectrum in the region of 3 μm together with the simulated spectra (stick spectra) for the most stable structures displayed on the right. The spectra have been recorded by monitoring the H_2 loss from the H_2-tagged complexes. The metal ion is shown as a purple circle.

For all the structures, one of the aromatic rings is folded over the DKP peptide ring and the other one is extended outwards, in a *trans* geometry allowing interaction with M^+. For the small cations, Li^+ and Na^+, the structure is close to that of the protonated dipeptide (Figures 1f and 1e), with the metal cation replacing the proton. Then the distance between the metal ion and the centre of the extended ring increases monotonously with the cation ionic radius and does not depend much on chirality (see Figure 3).

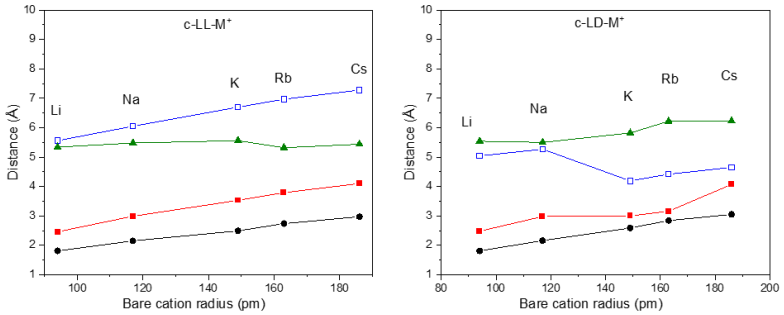

Figure 3: Geometrical parameters for the c-LL-M^+ (left) and the c-LD-M^+ (right) ion core complexes. Distance from M^+ to: oxygen amide atom (black full circle), centre of the extended ring (red full square), centre of the folded ring (blue empty circle). Distance between the centres of the two aromatic ring (green triangles).

However, c-LL-M^+ and c-LD-M^+ differ in that the cation only interacts with the amide oxygen and the extended ring in the c-LL-M^+ complexes. As a result, the metal ion remains in the amide plane for all c-LL-M^+ complexes. This is why the distance between the cation and each of the aromatic rings increases monotonously with the cation size and the inter-ring distance does not depend on the nature of the metal, nor does the angle between the aromatic rings, which are orthogonal to each other. In contrast, M^+ is located in-between the two aromatic rings in the c-LD-M^+ complexes and the metal cation interacts with both of them. The aromatic rings and the amide oxygen compete to interact with the cation and the cation departs from the amide plane to facilitate its simultaneous interaction with the two rings. Therefore, the distance between the metal ion and the centre of the two aromatic rings is dictated by the competition between the different interactions, which strongly depends on the metal.[19] For small ions, the metal is aligned with CO and mostly interacts with one ring. In contrast, for large ions, the ion is not collinear with CO and interacts with the two rings. As a result, the distance between M^+ and the extended ring increases with the ion size, while that between M^+ and the folded ring reaches a maximum for Na^+. Conversely, the inter-ring distance is minimal for Na^+. The angle between the aromatic rings also varies with the metal. While they are nearly perpendicular for small ions, they become almost parallel to each other for Cs^+, leading to a compact structure in which the cation is sandwiched by the two aromatic rings.

It is telling to compare the sensitivity of the spectroscopic signature to chirality, namely, the splitting between the two ν(NH) for c-LL-M^+ and c-LD-M^+, as a function of the metal ion (Figure 4). The difference between c-LL-M^+ and c-LD-M^+ is largest for Li^+ then decreases to reach zero for K^+ and changes sign. Figure 4 emphasises that the c-LL-K^+ and c-LD-K^+ complexes show very similar spectroscopic signatures. The same trend are observed for the ν(OH (not shown), although the frequency range is smaller.

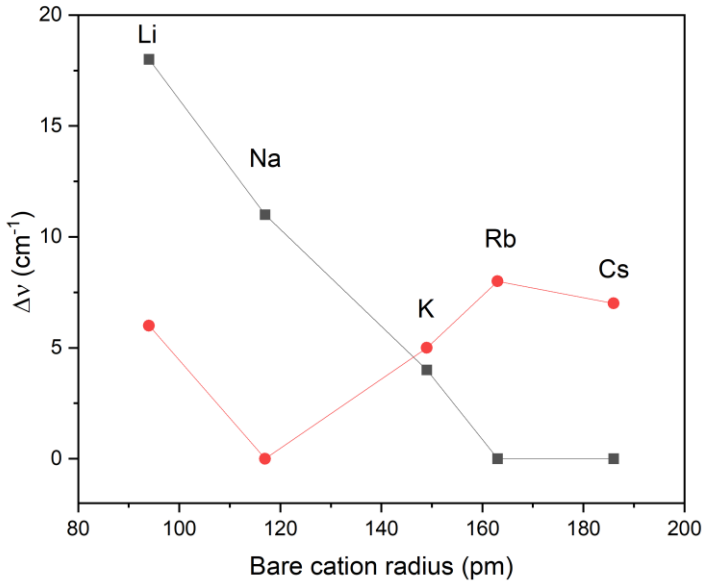

Figure 4: Dependence of the frequencies on chirality as a function of the metal ion. $\Delta\nu$ is the splitting between the ν(NH) located on the amide interacting with the metal ion and the ν(NH) located on the free amide. $\Delta\nu$ is shown by black squares for c-LL-M^+ and red circles for c-LD-M^+.

Vibrational Spectroscopy in the 6 μm Region.

Figure 5 shows the experimental spectra of the c-LL-M^+ and c-LD-M^+ ion core complexes in the 6 μm region, as well as those simulated for the most stable structures. Surprisingly, the spectrum shows three bands in the ν(CO) region, where only two bands are expected. To check whether the additional band results from the effect of the H_2 tag, IR-UV double resonance spectra have been recorded, setting the probe on the lower-energy UV transition (*vide infra*) on the example of the c-LL-K^+, c-LL-Cs^+, and c-LD-Cs^+ complexes (Figure S6 to S8). The lower-energy band is observed at the same frequency in the IR-UV and IRPD spectra, within 5 cm^{-1} and can be readily assigned to the ν(CO) interacting with the metal. The higher-energy band is also hardly modified between the IR-UV and IRPD spectra; it is assigned to the free ν(CO). The additional band at intermediate frequency is probably due to the effect of the H_2 tag and is likely to arise from a conformer with one H_2 molecule located close to the metal ion. In addition to that, a splitting of the free ν(CO) transition is observed in the IRPD spectrum of the c-LD-K^+ or c-LD-Li^+ complexes, as well as in the IR-UV spectrum of c-LD-Cs^+. The fact that this splitting is observed in the IR-UV spectrum of c-LD-Cs^+ and not in its IRPD spectrum points towards a Fermi resonance which is tuned on or off by the presence of the tag. To check this hypothesis, we have performed anharmonic calculations for the c-LD-Cs^+ complex. The obtained spectrum (Figure S9) indeed shows a splitting of the higher-energy band, which confirms this hypothesis.

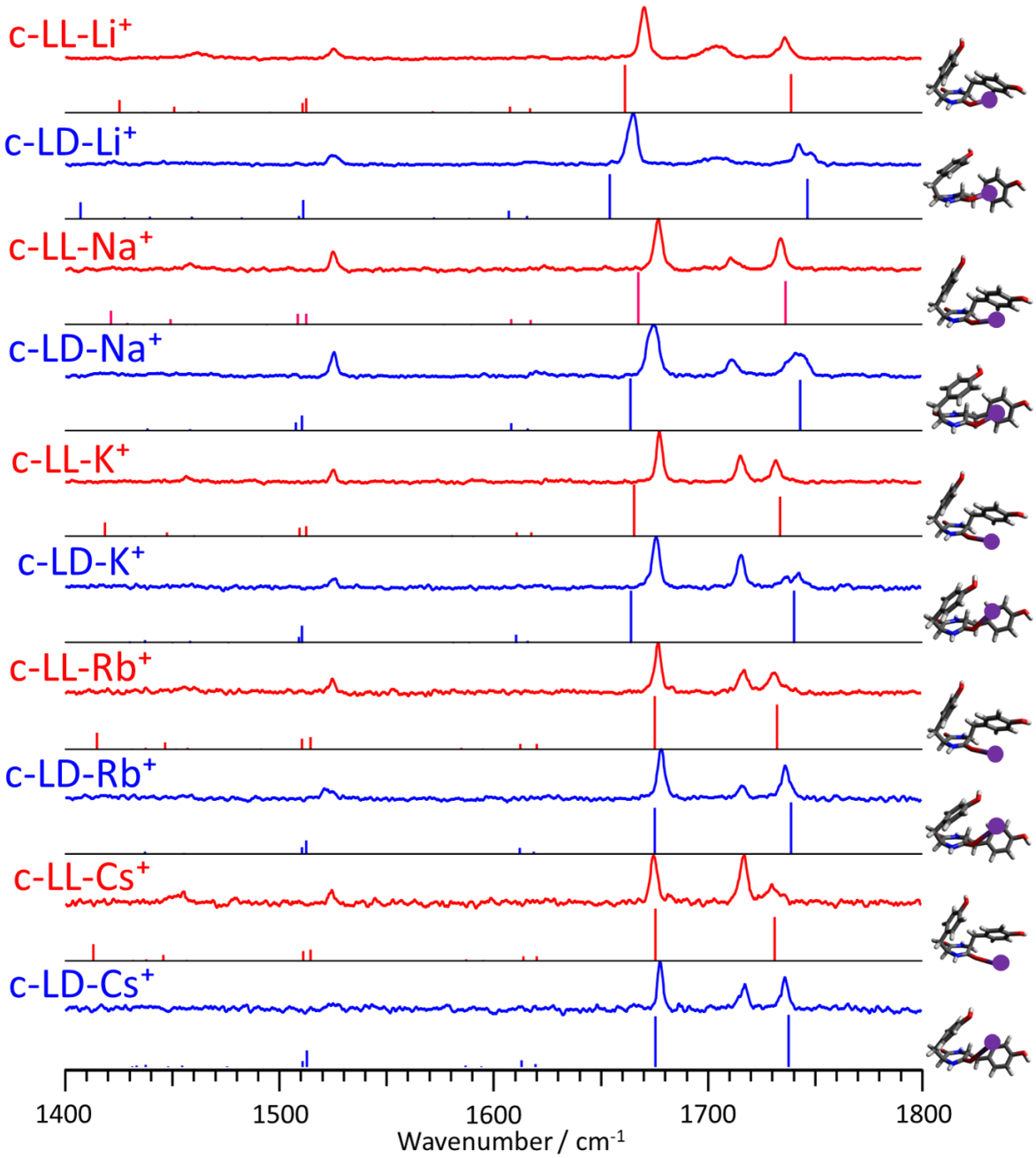

Figure 5: IR photodissociation spectra in the region of 6 μm together with the simulated spectra (stick spectra) for the most stable structures displayed on the right. The spectra have been recorded by monitoring the H_2 loss from the H_2-tagged complexes. The metal ion is shown as a purple circle.

Despite the large distance between the ion and the free amide, the frequency of the free ν(CO) decreases when the size of the cation increases, for both c-LL-M^+ and c-LD-M^+ complexes. The variation shows a quasi linear trend as a function of the electric field created by the ion (Figure S10). For the c-LD-M^+ complexes, the frequency of the bound ν(CO) smoothly increases when the size of the cation increases, reflecting both the increasing distance between the CO and the metal ion and the increasing competition between M^+…O and M^+…π interactions, which favours the latter for large ions. However, the dependence upon the electric field is far from being linear, in contrast to what was observed for the alkali-core polyglycine complexes.[33] The

shift from linearity is even more pronounced for the c-LL-M^+ complexes. The evolution of the bound ν(CO) of the latter is not even monotonous (see Figure S11), reflecting the fact that the interaction cannot be explained in electrostatic terms only.
The weaker feature at ~ 1525 cm^{-1} is assigned to the aromatic in-plane β(CH); it is not sensitive to chirality nor to the size of the metal cation and will not be discussed further.

Electronic Spectroscopy.

The UVPD electronic spectra of all the ion core complexes are shown in Figure 6. The spectra of the K^+, Rb^+, Cs^+ complexes have been recorded by monitoring the mass of the metal ion fragment as a function of the UV wavelength and that of the Li^+ and Na^+ complexes by monitoring the mass of a molecular ion fragment, namely, *m/z* 119. We shall come back to the specific fragmentation pattern later.

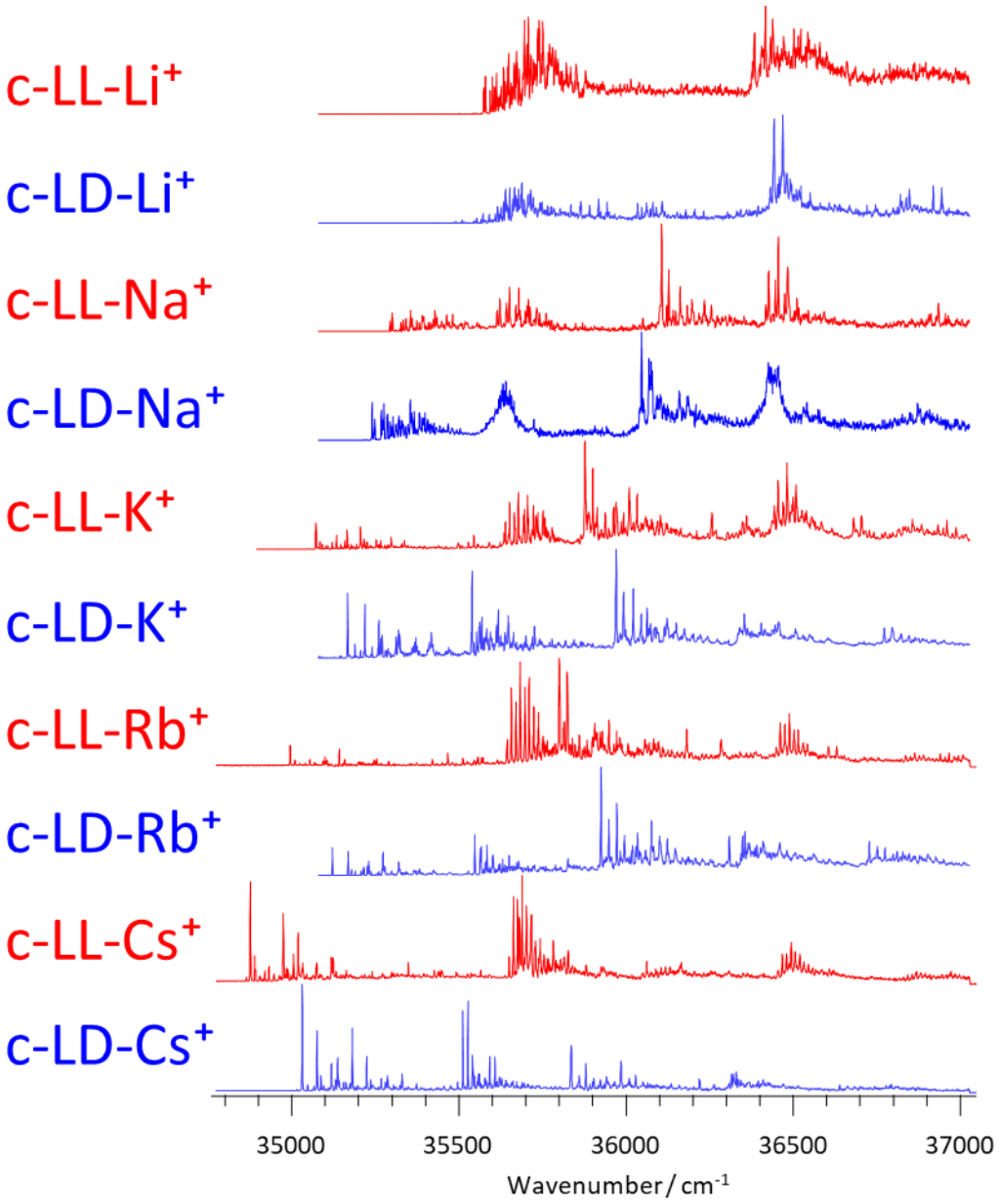

Figure 6: UV photo-dissociation spectra of the ion core complexes. The c-LL-M^+ complexes are shown in red and the c-LD-M^+ in blue. The spectra of the Li^+ and Na^+ ion core complexes have been obtained by monitoring the fragments *m/z* 119 and *m/z* 220, respectively. The spectra of the other complexes have been recorded by monitoring the M^+ loss (see text).

For a given absolute configuration of the residues, namely, LL or LD, the transition origin is shifted down in energy when the size of the cation increases. This is reminiscent of what was observed in a series of jet-cooled ion pairs based on the phenylacetate chromophore and the very same alkali metal cations as studied here,[34] or for the dimethoxy-benzene ion core complexes.[35] The increase of the red shift of the electronic transition was then explained in terms of an intramolecular Stark effect due to the electric field caused by the ion on the aromatic ring.[34] The c-LL-Li^+ and c-LD-Li^+ transition origins are located very close to that of bare tyrosine (35941 to 35650 cm^{-1} depending on the conformer).[36] For the Li^+ and Na^+ ion core complex, the electronic transition of c-LD-M^+ is lower in energy than that of c-LL-M^+. It is the opposite from K^+ on, with a difference that increases with the size of the metal ion. Interestingly, the change in ordering between the electronic transitions energies happens between K^+ and Na^+, as it was the case for the vibrational frequencies of ν(NH). This effect is difficult to rationalise but it could be due to the fact that the two benzene rings are roughly orthogonal to each other in all the c-LL-M^+ complexes, while the geometry changes as a function of the ion size in the c-LD-M^+ complexes. While it resembles that of c-LL-M^+ with orthogonal benzene rings for Li^+ and Na^+, it evolves to a more parallel (V shape) structure for larger ions. The change happens for K^+, which could explain the changes in spectroscopic signature observed for this ion.

Figure 7 shows the vertical transition energies for the first six $S_n \leftarrow S_0$ electronic transitions.

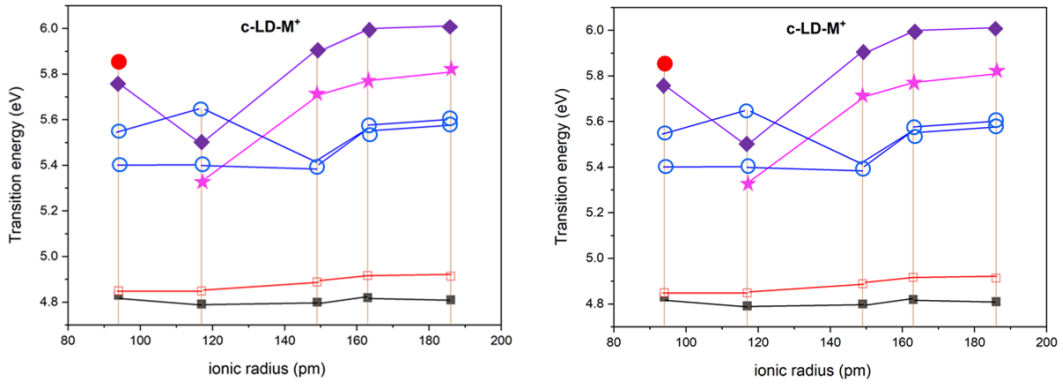

Figure 7: Ordering of the electronic transitions $S_n \leftarrow S_0$. Full black squares: $\pi\pi^*$ transition located on the extended ring. Empty red squares: $\pi\pi^*$ transition located on the folded ring. Full magenta stars: charge transfer from the extended aromatic ring to the metal ion. Blue empty circle: transitions located on the peptide ring. Full purple lozenges: charge transfer from the folded aromatic ring to the metal ion. Full red circles: charge transfer from the folded aromatic ring to the extended one.

Geometry optimisation of the excited states is beyond the scope of this article and we shall discuss the results on the basis of vertical transition energies. The electron density difference

between the electronic ground state S_0 and selected electronic excited states S_n are shown in Figure 8. For all the ion-core complexes, the $S_1 \leftarrow S_0$ and $S_2 \leftarrow S_0$ transitions are $\pi\pi^*$ transitions localised on the extended and folded benzene rings, respectively, as it was already the case for the neutral molecule.[17] Figures 8a and 8b show these transitions on the example of c-LL-Li^+. The transitions located on the amide (Figures 8c) show little variation with the ion core or with chirality. The CT from the folded ring to the metal ion (Figures 8d) is high in energy for all the systems and will not be discussed further. The vertical energy and the nature of the other $S_n \leftarrow S_0$ transitions depend on both the metal ion and the relative chirality of the residues, as summarised in Figure 7.

For the c-LL-M^+ complexes, the $S_3 \leftarrow S_0$ transition always has a charge transfer (CT) character. For all c-LL-M^+ complexes but c-LL-Li^+, it corresponds to a CT from the extended ring to the metal, similar to that depicted in Figure 8e on the example of c-LD-Rb^+. Its energy raises when the size of the metal ion increases and so does the separation between $S_3 \leftarrow S_0$ and $S_1 \leftarrow S_0$ or $S_2 \leftarrow S_0$. The influence of this CT states is thus expected to become smaller when the size of the metal cation increases and is thus maximum for Na^+. Among the c-LL-M^+ complexes, c-LL-Li^+ stands out in that no CT transition from an aromatic ring to Li^+ are calculated among the first 6 electronic transitions. Instead, intramolecular CT from the folded to the extended aromatic ring is calculated at low energy and is the $S_3 \leftarrow S_0$ transition (Figures 8f). Such a transition is also calculated as $S_5 \leftarrow S_0$ in c-LL-Na^+.

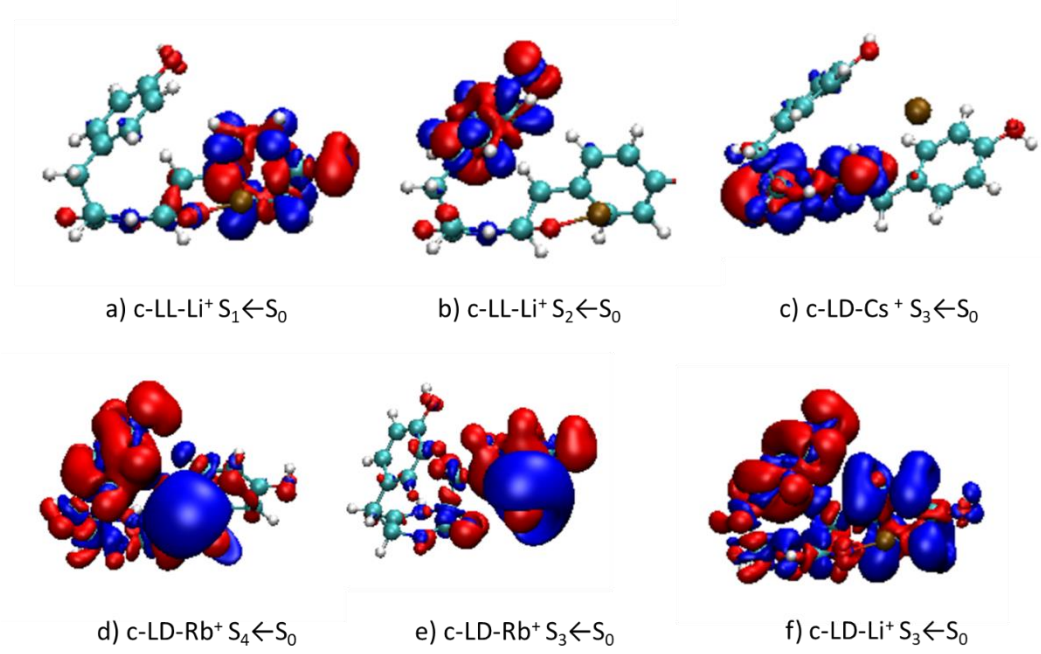

Figure 8: Electron density difference between the electronic ground state S_0 and selected electronic excited states S_n (see text). The cut-off is set at 0.001. Positive values, shown in blue, correspond to an increase of the electron density in S_n. Negative values, shown in red, correspond to a decrease of the electron density in S_n.

The situation is very different for the c-LD-M^+ complexes. The CT between the benzene rings exists for Li^+ only. The transitions located on the amides are low in energy and correspond to $S_3 \leftarrow S_0$ and $S_4 \leftarrow S_0$ for all systems but Na^+. The CTs to the ion, similar to those described in the c-LL-M^+ complexes are very high in energy, except for Na^+ where it corresponds to $S_3 \leftarrow S_0$. c-LD-Na^+ therefore differs from the other c-LD-M^+ complexes by the fact that the $S_3 \leftarrow S_0$ transition is a charge transfer from the extended aromatic ring to the metal ion. In both c-LL-Na^+ and c-LD-Na^+, the CT from the extended aromatic ring to the metal ion is very low in energy, compared to the other metal ion complexes, which points towards specific photophysical behaviours of Na^+.

We can now discuss the experimental results at the light of these theoretical findings. Among the c-LL-M^+ complexes, c-LL-Li^+ stands out in that it has a low-energy intramolecular CT between the benzene rings ($S_3 \leftarrow S_0$ transition). This is in line with the UVPD spectrum of c-LL-Li^+ that shows a broad absorption superimposed with the narrow transitions. This broad absorption could result from the presence of the above-mentioned CT state. From Na^+ on, the $S_3 \leftarrow S_0$ c-LD-M^+ is a CT to the metal whose energy raises when the size of the metal ion increases, which might explain the broad absorption observed in the UVPD spectrum of c-LD-Na^+ and not for the other ions.

The calculations also allow rationalising the fragments obtained by photo-dissociation. The mass spectra resulting from the excitation of the origin transition of the c-LL-M^+ complexes are shown in Figure 9.

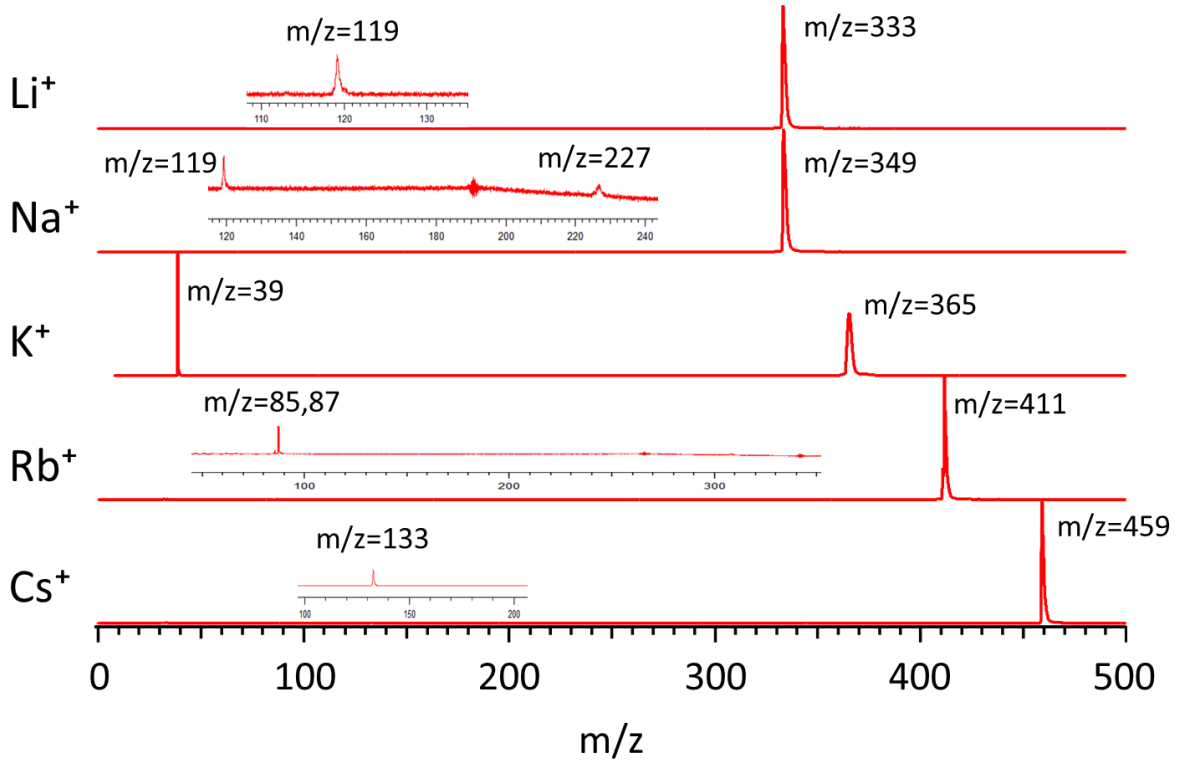

Figure 9: MS^2 spectrum resulting from the excitation of the transition origin of the c-LL-M^+ complexes. The insert is a zoom by a factor of 50.

For K^+, Rb^+, and Cs^+, the fragment is the metal ion, which suggests internal conversion to the ground state and intermolecular fragmentation. The observation of the M^+ fragment is in line with the fact that the CT states from an aromatic ring to the cation are high in energy for K^+, Rb^+, and Cs^+. The fragment would not be M^+ if the S_3 CT state crossed the optically excited state because CT corresponds to a reduction of the metal ion and a neutral metal should be formed. In contrast, a molecular fragment at *m/z* 119 is observed for the Li^+ and Na^+ complexes. This fragment has been observed already in the collision-induced dissociation of cyclo(prolyl-tyrosyl)H^+. It is explained in terms of the heterolytic cleavage of the DKP ring leading to the loss of the quinopropyl radical ion $CH_2CHC_6H_4O^+$. Interestingly, the *m/z* 119 fragment is only observed for Li^+ and Na^+ and not the other metal ions, pointing towards a specific fragmentation pattern for the electronic excited states of the Li^+ and Na^+ complexes. Conversely, the Na^+ and Li^+ fragments are not observed for the UVPD of the corresponding complexes. Although we cannot draw definite conclusions for Li^+, the small mass of which makes it difficult to detect, it would be possible to detect Na^+ should if it were produced. Thus, Na^+ does not appear as a photoproduct of the c-LL-Na^+ and c-LD-Na^+ complexes.

The presence of low-lying CT states explains the peculiar fragmentation pattern observed for the Li^+ and Na^+ complexes. The CT state involves indeed charge transfer to the metal ion, thus its reduction to a neutral species. The reduction of the metal is accompanied by the migration of the charge on the dipeptide, resulting to the formation of *m/z* 119 with localisation of the charge on the C_8H_7O fragment. This is reminiscent of what was reported for Ag^+ core peptides where sequential proton and electron transfer has been observed.[37] The presence in the MS^2 spectrum of c-LL-Na^+ of the weak and broad band at *m/z* 227 is more difficult to rationalise. It can be tentatively explained by the cleavage of the DKP ring accompanied by proton transfer, which results in the loss of the close-shell $CH_3CH_2C_6H_4OH$ molecular fragment (M=122) and an ionic fragment still containing the metal ion. The mechanisms are summarised in Figure 10.

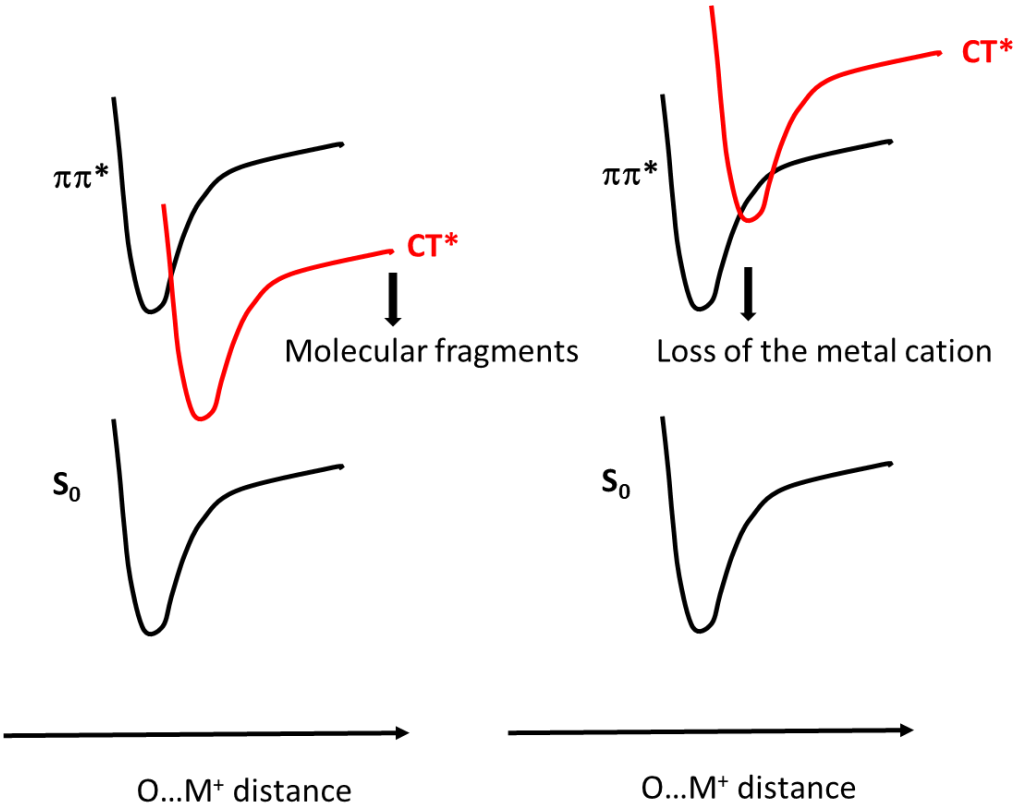

Figure 10: Schematic view of the deactivation processes depending on the position of the charge transfer state. Na^+ complexes (left) and larger cation core complexes (right).

The geometry of the S_1, S_2, and S_3 transitions has been optimised for c-LL-Na^+. While the geometry of the optimised S_2 and S_3 states does not change much compared to that of the ground state, the S_1 state is stabilised by almost 10,000 cm^{-1}, with an important change in the O…Na^+ distance upon electronic excitation (see Figure S11). This suggests that the charge transfer transition becomes lower in energy than that of the ππ* transitions at the equilibrium geometry and confirms the role of the charge transfer states in the photo-physics of the Na^+ complexes.

Conclusion

Vibrational spectroscopy combined with quantum chemical calculations have been used to shed light on the structure of the cylo-Tyr-Tyr ion core complexes with alkali metal. We have shown that the structural motif depends on both the metal cation and the relative chirality of the tyrosine residues. In all the studied systems, the metal ion binds to one of the amide oxygen atoms. The structure of the c-LL-M^+ complexes has one ring folded over the peptide ring, whose position does not change with the size of the cation, and the other one extended, which allows interaction with the metal ion (Oπ type interaction). The c-LL-M^+ complexes show a monotonous dependence of the M^+…O and M^+…extended ring distances upon the size of the metal ion and a constant distance between the aromatic rings. The structural pattern of the c-LD-M^+ complexes are more diverse; they are dictated by the balance between the interaction of the metal ion with the amide oxygen, the extended ring, and the folded ring. As

a result, the two aromatic rings, which are perpendicular to each other for the c-LD-Li^+ and c-LD-Na^+ complexes, become parallel for larger metal ions, sandwiching the cation. This is reminiscent of the cation π cage observed for diphenylalanine ion core complexes.[22] The formation of such a fully solvated structure is here facilitated by the conjunction between the cyclic nature of the peptide and steric constraints due to chirality that facilitate this interaction in c-LD-M^+ only and not in c-LL-M^+. The difference between c-LL-M^+ and c-LD-M^+ depends on the cation size. The c-LL-M^+ *vs.* c-LD-M^+ difference in splitting between the two ν(NH) evolves with the cation size and is almost zero for K^+, then changes sign. The same inversion at K^+ is also observed for the electronic transitions: that of c-LD-M^+ is lower in energy for Li^+ and Na^+ than it is the opposite. Among the studied complexes, those with Na^+ stand out due to specific Na^+ induced stabilization of a charge transfer state from the extended aromatic ring to the cation, which induces broadening of the UVPD spectrum in the case of c-LD-Na^+ and dissociation towards molecular fragments. This study emphasises the fact that the differences between two diastereomers of a cyclic dipeptide can be either emphasised or blurred upon complexation with an alkali metal ion, depending on the metal size.

Acknowledgements

A.Z. acknowledges travel support from the World Research Hub Initiative (WRHI) of Tokyo Institute of Technology. This work was supported in part by KAKENHI (JP19K23624, JP20K20446, JP20H00372, JP21H04674, and JP21K14585) of JSPS, World Research Hub Initiatives in Tokyo Institute of Technology, the Cooperative Research Program of the "Network Joint Research Centre for Materials and Devices" and Core-to-Core Program (JPJSCCA20210004) from the Ministry of Education, Culture, Sports, Science and Technology (MEXT), Japan, and the RIKEN Pioneering Project, "Fundamental Principles Underlying the Hierarchy of Matter: A Comprehensive Experimental Study". The computations were performed at the Research Centre for Computational Science, Okazaki, Japan (21-IMS-C109) and the MAGI HPC computing centre (Université Paris Cité) and the MESOLUM cluster (Université Paris Saclay).

Keywords

Chirality – Cryogenic ion trap – Diketopiperazine – Dipeptides – Laser Spectroscopy

References

[1] N. M. Kidwell, B. Nebgen, L. V. Slipchenko, T. S. Zwier *Journal of Chemical Physics*. **2019**, *151*, 084313.
[2] S. Kopec, P. Ottiger, S. Leutwyler, H. Koppel *Journal of Chemical Physics*. **2015**, *142*, 084308.
[3] N. S. Nagornova, T. R. Rizzo, O. V. Boyarkin *Journal of the American Chemical Society*. **2010**, *132*, 4040-4041.
[4] A. Zehnacker, F. Lahmani, E. Breheret, J. P. Desvergne, H. BouasLaurent, A. Germain, V. Brenner, P. Millie *Chemical Physics*. **1996**, *208*, 243-257.
[5] C. Prasad *Peptides*. **1995**, *16*, 151-164.

[6] I. Bellezza, M. J. Peirce, A. Minelli *Trends in Molecular Medicine*. **2014**, *20*, 551-558.
[7] K. Yoshizawa, K. Hirata, S. I. Ishiuchi, M. Fujii, A. Zehnacker *Journal of Physical Chemistry A*. **2022**, *126*, 6387-6394.
[8] A. F. Perez-Mellor, R. Spezia, A. Zehnacker *Symmetry-Basel*. **2022**, *14*, 679.
[9] K. Le Barbu-Debus, A. Perez-Mellor, V. Lepere, A. Zehnacker *Physical Chemistry Chemical Physics*. **2022**, *24*, 19783-19791.
[10] J. Dupont, R. Guillot, V. Lepère, A. Zehnacker *Journal of Molecular Structure*. **2022**, *1262*, 133059.
[11] A. Pérez-Mellor, K. Le Barbu-Debus, V. Lepere, I. Alata, R. Spezia, A. Zehnacker *The European Physical Journal D*. **2021**, *75*, 165.
[12] A. Pérez-Mellor, I. Alata, V. Lepère, R. Spezia, A. Zehnacker-Rentien *International Journal of Mass Spectrometry*. **2021**, *465*, 116590.
[13] A. Pérez-Mellor, I. Alata, V. Lepère, A. Zehnacker *The Journal of Physical Chemistry B*. **2019**, *123*, 6023-6033.
[14] A. Pérez Mellor, A. Zehnacker in *Chirality Effects in Jet-Cooled Cyclic Dipeptides, Vol.* (Eds.: T. Ebata, M. Fujii), Springer, Singapore, **2019**, pp.63-87.
[15] A. Pérez-Mellor, I. Alata, V. Lepere, A. Zehnacker *Journal of Molecular Spectroscopy*. **2018**, *349*, 71-84.
[16] I. Alata, A. Pérez-Mellor, F. Ben Nasr, D. Scuderi, V. Steinmetz, F. Gobert, N. E. Jaïdane, A. Zehnacker-Rentien *The Journal of Physical Chemistry A*. **2017**, *121*, 7130-7138.
[17] F. BenNasr, A. Pérez-Mellor, I. Alata, V. Lepere, N. E. Jaidane, A. Zehnacker *Faraday Discussions*. **2018**, *212*, 399-419.
[18] B. A. Cerda, S. Hoyau, G. Ohanessian, C. Wesdemiotis *Journal of the American Chemical Society*. **1998**, *120*, 2437-2448.
[19] R. C. Dunbar, G. Berden, J. Oomens *International Journal of Mass Spectrometry*. **2013**, *354–355*, 356-364.
[20] N. C. Polfer, J. Oomens, R. C. Dunbar *ChemPhysChem*. **2008**, *9*, 579-589.
[21] R. Otsuka, K. Hirata, Y. Sasaki, J. M. Lisy, S. Ishiuchi, M. Fujii *ChemPhysChem*. **2020**, *21*, 712-724.
[22] R. C. Dunbar, J. D. Steill, J. Oomens *Journal of the American Chemical Society*. **2011**, *133*, 9376-9386.
[23] R. C. Dunbar, J. D. Steill, J. Oomens *Journal of the American Chemical Society*. **2011**, *133*, 1212-1215.
[24] V. Lepere, K. Le Barbu-Debus, C. Clavaguéra, D. Scuderi, G. Piani, A.-L. Simon, F. Chirot, L. MacAleese, P. Dugourd, A. Zehnacker *Physical Chemistry Chemical Physics*. **2016**, *18*, 1807-1817.
[25] S. Ishiuchi, H. Wako, D. Kato, M. Fujii *Journal of Molecular Spectroscopy*. **2017**, *332*, 45-51.
[26] J. Donon, J.-X. Bardaud, V. Brenner, S.-I. Ishiuchi, M. Fujii, E. Gloaguen *Phys. Chem. Chem. Phys.* **2022**, *24*, 12121-12125.
[27] M. J. Frisch, J. A. Pople, J. S. Binkley *Journal of Chemical Physics*. **1984**, *80*, 3265-3269.
[28] S. Grimme, J. Antony, S. Ehrlich, H. Krieg *Journal of Chemical Physics*. **2010**, *132*, 154104
[29] S. Grimme, S. Ehrlich, L. Goerigk *Journal of Computational Chemistry*. **2011**, *32*, 1456-1465.
[30] M. J. Frisch, G. W. Trucks, H. B. Schlegel, G. E. Scuseria, M. A. Robb, J. R. Cheeseman, G. Scalmani, V. Barone, G. A. Petersson, H. Nakatsuji, X. Li, M. Caricato, A. V. Marenich, J. Bloino, B. G. Janesko, R. Gomperts, B. Mennucci, H. P. Hratchian, J. V. Ortiz, A. F. Izmaylov, J. L. Sonnenberg, Williams, F. Ding, F. Lipparini, F. Egidi, J. Goings, B. Peng, A. Petrone, T. Henderson, D. Ranasinghe, V. G. Zakrzewski, J. Gao, N. Rega, G. Zheng, W. Liang, M. Hada, M. Ehara, K. Toyota, R. Fukuda, J. Hasegawa, M. Ishida, T. Nakajima, Y. Honda, O. Kitao, H. Nakai, T. Vreven, K. Throssell, J. A. Montgomery Jr., J. E. Peralta, F. Ogliaro, M. J. Bearpark, J. J. Heyd, E. N. Brothers, K. N. Kudin, V. N. Staroverov, T. A. Keith, R. Kobayashi, J. Normand, K. Raghavachari, A. P. Rendell, J. C. Burant, S. S. Iyengar, J. Tomasi, M. Cossi, J. M. Millam, M. Klene, C. Adamo, R. Cammi, J. W. Ochterski, R. L. Martin, K. Morokuma, O. Farkas, J. B. Foresman, D. J. Fox in Gaussian 16 Rev. B.01, **2016**.
[31] F. Weigend, M. Haser *Theoretical Chemistry Accounts*. **1997**, *97*, 331-340.
[32] W. Humphrey, A. Dalke, K. Schulten *J. Molec. Graphics*. **1996**, *14*, 33-38.

[33] K. A. E. Meyer, K. A. Nickson, E. Garand *Journal of Chemical Physics*. **2022**, *157*, 113107.
[34] J. Donon, S. Habka, V. Vaquero-Vara, V. Brenner, M. Mons, E. Gloaguen *Journal of Physical Chemistry Letters*. **2019**, *10*, 7458-7462.
[35] Y. Inokuchi, O. V. Boyarkin, T. Ebata, T. R. Rizzo *Physical Chemistry Chemical Physics*. **2012**, *14*, 4457-4462.
[36] Y. Shimozono, K. Yamada, S. Ishiuchi, K. Tsukiyama, M. Fujii *Physical Chemistry Chemical Physics*. **2013**, *15*, 5163-5175.
[37] L. MacAleese, S. Hermelin, K. El Hage, P. Chouzenoux, A. Kulesza, R. Antoine, L. Bonacina, M. Meuwly, J.-P. Wolf, P. Dugourd *Journal of the American Chemical Society*. **2016**, *138*, 4401-4407.

Alkali metal complexes of the cyclic dipeptide cyclo Tyr-Tyr isolated in a cryogenic ion trap show a structural motif that strongly depends on the relative chirality of the tyrosine residues and on the size of the metal ion.